A&A 474, 923–930 (2007)
DOI: 10.1051/0004-6361:20078138

Astronomy & Astrophysics

The fractional ionization in dark molecular clouds

D. R. Flower[1], G. Pineau des Forêts[2,3], and C. M. Walmsley[4]

[1] Physics Department, The University, Durham DH1 3LE, UK
e-mail: david.flower@durham.ac.uk
[2] Institut d'Astrophysique Spatiale (IAS), UMR 9617 CNRS, Bâtiment 121, 91405 Orsay, France
[3] LERMA (UMR 8112 CNRS), Observatoire de Paris, 61 avenue de l'Observatoire, 75014 Paris, France
[4] INAF, Osservatorio Astrofisico di Arcetri, Largo Enrico Fermi 5, 50125 Firenze, Italy

Received 22 June 2007 / Accepted 23 August 2007

ABSTRACT

Aims. We have studied the mechanisms which govern the degree of ionization of the gas in molecular clouds and prestellar cores, with a view to interpreting the relative abundances of the carbon-chain species C_nH and their negative ions, C_nH^-.
Methods. We followed the chemical evolution of a medium comprising gas and dust as it evolves towards its steady-state composition. Various assumptions were made concerning the grain size-distribution and the fraction of very small grains (in practice, PAH), as well as the cosmic ray ionization rate. Particular attention was paid to reactions which determine the fractional ionization of the gas and the charge of the grains.
Results. We found that the abundance ratio $n(C_6H^-)/n(C_6H)$ is determined essentially by the ratio of the free electron density to the density of atomic hydrogen. A model with a high fractional abundance of PAH and a low fractional abundance of electrons yields agreement to a factor of 2 with the value of the ratio C_6H^-:C_6H observed recently in TMC-1. However, the fractional abundances of the molecular ions HCO^+ and DCO^+ are then higher than observed. The best overall fit with the observations of TMC-1 is obtained when the cosmic ray ionization rate is reduced, together with the rate of removal of atomic hydrogen from the gas phase (owing to adsorption on to grains).

Key words. astrochemistry – molecular processes – stars: formation – ISM: clouds – ISM: molecules – radio lines: ISM

1. Introduction

The observational determination of the degree of ionization of the gas in the molecular clouds from which stars form has proved to be an elusive goal. However, recent observations of the negative ions of the carbon-chain species C_6H and C_8H (in TMC-1, and also in IRC 10216; McCarthy et al. 2006; Brünken et al. 2007; Remijan et al. 2007) and C_4H (in IRC 10216; Cernicharo et al. 2007) raise the prospect that the ratio of the column densities of the anions (C_nH^-) and the corresponding molecules (C_nH) might be related to, and perhaps provide a measure of, the fractional abundance of electrons in the molecular gas. This expectation was one of the original motivations for the present study.

Positive charge is carried mainly by atomic and molecular ions ("cations"), whereas negative charge is carried by grains – including the "very small grains" (VSG), which we shall identify with polycyclic aromatic hydrocarbons (PAH) – by negative ions ("anions") and by free electrons. The interaction of these various forms of charged particle with a magnetic field, which can play an important role in gravitational collapse, depends on their inertia and hence on both number density and mass. It seems unlikely that observations will ever be able to provide all the information required to quantify this interaction, and some reliance will continue to be placed on chemical models of the medium.

In the early stages of formation of low-mass stars, the freeze-out of atoms and molecules on to the surfaces of dust grains is likely to have profound consequences for the composition of the gas-phase material. There is evidence (e.g. Cardelli et al. 1989; Ossenkopf 1993; Ossenkopf & Henning 1994; Suttner & Yorke 2001) that grains, and possibly PAH, may undergo significant coagulation before the onset of the gravitational collapse proper. In this case, the adoption of the Mathis et al. (1977, hereafter MRN) grain size-distribution, which was established from observations of the diffuse interstellar medium, is inappropriate. The key parameter, from the standpoint of gas-grain interactions in general, and the freeze-out of the gas-phase species in particular, is the mean value of $(n_g/n_H)\sigma_g$, where n_g is the grain number density, $\sigma_g = \pi a_g^2$ is the grain (assumed spherical) cross section and $n_H \approx n(H) + 2n(H_2)$ is the total number density of hydrogen nuclei. An MRN size distribution yields a value of the mean grain cross section per hydrogen nucleus[1], $(n_g/n_H)\pi a_g^2 = 1.6 \times 10^{-21}$ cm^2, corresponding to a grain radius $a_g = 0.05$ μm (see below). On the other hand, grains which have coagulated have a smaller mean cross section. For example, a grain radius $a_g = 0.5$ μm corresponds to $(n_g/n_H)\pi a_g^2 = 1.6 \times 10^{-22}$ cm^2; this value of the cross section has been found to be compatible with the observed differential freeze-out of carbon- and nitrogen-containing species in the early phases of protostellar collapse (Flower et al. 2006b).

The mean grain cross section per hydrogen nucleus is important not only for the interactions of the gas with the grains but also for the absorption of the ultraviolet radiation. Even in the absence of local sources of radiation and of the background interstellar field, owing to screening by the surrounding dust, ultraviolet radiation is produced by the interactions of

[1] The quantity $(n_g/n_H)\pi a_g^2$ has come to be known as "the mean grain cross section per hydrogen nucleus". We note that it should be more appropriately called "the mean grain opacity per hydrogen nucleus" and is the product of the mean grain cross section and the fractional abundance of the grains.

cosmic rays (CR), principally with molecular hydrogen (Prasad & Tarafdar 1983). The secondary electrons, generated by

$$H_2 + CR \rightarrow H_2^+ + e^-$$

and

$$H_2 + CR \rightarrow H^+ + H + e^-$$

have a mean kinetic energy of approximately 30 eV (Cravens & Dalgarno 1978). These electrons can excite the Lyman, Werner and other bands of the H_2 molecules in the medium, generating ultraviolet photons in the subsequent radiative cascade back to the $X^1\Sigma_g^+$ electronic ground state; these photons are then available to ionize and dissociate other species. The rates of photodissociation and photoionization are dependent on the relative numbers of photons which are absorbed by the gas and by the dust. If the dust is assumed to have an MRN size distribution, and an albedo of about 0.5, most of the photons are, in fact, absorbed by the dust and (depending on its fractional abundance) CO (Gredel et al. 1987). However, larger grains absorb a smaller fraction of the ultraviolet photons, and this should be taken into account when evaluating the ionization and dissociation rates.

TMC-1 was the first molecular cloud core in which long-chain carbon species were discovered (Morris et al. 1976), and it has been used subsequently to test models of the formation of large "organic" species (Millar et al. 2000). TMC-1 seems to be unusual, in respect of both the high fractional abundances of long-chain carbon species and the low degree of deuterium enrichment of HCO^+ (Caselli et al. 1998). As the timescale for converting carbon into CO is relatively long, these observations have been interpreted as being indicative of the youth of this core. It will be seen below that our analysis of the observed C_6H^-:C_6H ratio suggests that the cosmic ray ionization rate in this core may also be unusually low, with consequences for simulations of the organic chemistry in TMC-1.

In Sect. 2, we outline the model that has been used in the present study, with the emphasis being placed on those processes which modify the charge distribution in the medium. Section 3 contains the main results of our calculations, notably regarding the diagnostic potential of the $n(C_nH^-)/n(C_nH)$ abundance ratios. Our concluding remarks are to be found in Sect. 4.

2. The model

In this section, we describe the model that we have used in our study. The main thrust of our work was to calculate as accurately as possible the degree of ionization of the gas and the distribution of negative charge in the medium. One facet of the analysis relates to ionization (and dissociation) of molecules and ionization of atoms by the ultraviolet radiation field which is generated in a molecular medium, following cosmic ray ionization of H_2. There has been some confusion in the literature regarding the rates for these processes, and so we present, in Appendix A, our treatment of this mechanism.

The elemental abundances, in the gas phase (and their fractional depletion on to grains), were as follows: C 8.27×10^{-5} (0.77); N 6.39×10^{-5} (0.20); O 8.49×10^{-5} (0.79); S 6.00×10^{-7} (0.97); Fe 1.50×10^{-9} (1.00).

2.1. C_nH^-

As intimated in the Introduction, the measurement of the column densities of both the neutral and negatively charged forms of the carbon-chain species C_nH ($n = 4, 6$) might be expected to yield information on the electron density in dark clouds. Electron attachment reactions lead to the formation of the negative ion, which is removed by electron detachment in reactions with neutrals, principally atomic hydrogen, and by mutual neutralization reactions with positive ions. For electron attachment to the corresponding linear carbon clusters, C_4 and C_6, Terzieva & Herbst (2000) calculated rate coefficients of $1.4 \times 10^{-8}(T/300)^{-0.5}$ and $1.7 \times 10^{-7}(T/300)^{-0.5}$ cm^3 s^{-1}, respectively. The results of Terzieva & Herbst (2000) incorporated an electron attachment probability per collision of 0.08 for C_4 and of 1.0 for C_6. On the other hand, in a recent study of formation of the anions of C_nH, Millar et al. (2007) indicate that, for $n = 4$, the attachment probability is only around 1%. Accordingly we have used a rate coefficient of $1.7 \times 10^{-9}(T/300)^{-0.5}$ cm^3 s^{-1} for electron attachment to C_4H. Eric Herbst has informed us that the probability of electron attachment to C_6H is high in the singlet electron spin entrance channel, which, statistically, is followed by 1/4 of the collisions (with 3/4 of the scattering events being in the triplet spin channel). Accordingly, we adopted a rate coefficient for electron attachment to C_6H of $4.3 \times 10^{-8}(T/300)^{-0.5}$ cm^3 s^{-1}.

The dominant removal process is

$$C_nH^- + H \rightarrow C_nH_2 + e^-,$$

for which we have used the rate coefficients of 8.3×10^{-10} and 5.0×10^{-10} cm^3 s^{-1}, for $n = 4$ and $n = 6$, respectively, as measured by Barckholtz et al. (2001). Reactions with other neutral species and with cations, although included in the reaction set, are less significant, owing to the lower fractional abundances of these reactants.

There are no data on electron attachment and detachment specific to C_8H^-. A reasonable assumption might be that the rate coefficients for the formation and destruction of C_8H^- are similar to those for C_6H^-, in which case the abundance ratios C_8H^-:C_8H and C_6H^-:C_6H should also be similar.

Under the conditions in dark clouds, which are shielded from the external radiation field by dust, electron attachment tends to dominate the formation and electron detachment by H the destruction of C_6H^-, the ratio of the abundances of C_6H^- and C_6H in steady state at $T = 10$ K is given by

$$\frac{n(C_6H^-)}{n(C_6H)} = 4.7 \times 10^2 \frac{n_e}{n(H)},$$

where n_e is the electron number density and $n(H)$ is the number density of atomic hydrogen; the factor of 4.7×10^2 is the ratio of the rate coefficients for the formation and destruction of C_6H^-, evaluated at $T = 10$ K. The density of H is determined essentially by its production in the dissociation of H_2 by cosmic rays and its removal in the formation of H_2 on grains. Assuming an MRN grain size distribution and a kinetic temperature $T = 10$ K, the density of H is given by

$$n(H) = 2.2 \times 10^{16} \zeta,$$

where ζ (s^{-1}) is the rate of cosmic ray ionization, defined in Appendix A below, and $n(H)$ is expressed in cm^{-3}. The density of H is larger, by a factor of 10, if a mean grain cross section per hydrogen nucleus $(n_g/n_H)\pi a_g^2 = 1.6 \times 10^{-22}$ cm^2 is adopted, owing to the reduced rate of formation of H_2 (and removal of H).

The electron density is the difference between the total abundances of the cations and of the anions. The latter include PAH^- and, depending on the fractional abundance of the PAH, n_{PAH}/n_H (see Sect. 2.2 below), can be the small difference between two much larger numbers. As the electron affinities of both C_6H and C_4H (Taylor et al. 1998) are larger than those of the PAH

(Modelli & Mussoni 2007), electron transfer from PAH^- to C_6H and C_4H is energetically possible and has been included in our reaction set with a rate coefficient of 1.7×10^{-9} cm^3 s^{-1}. However, as will be seen in Sect. 3.2, the key factors determining the ratio $n(C_6H^-)/n(C_6H)$ are the free electron density and the density of atomic hydrogen.

In the limit of a negligible PAH abundance, the total number density of positive ions is equal to the density of free electrons. Then, the rate of removal of electrons, through recombinations with positive ions, is proportional to n_e^2, and the rate of creation of electrons, through cosmic ray ionization of hydrogen, is proportional to ζn_H. Thus, in steady state, $n_e \propto (\zeta n_H)^{0.5}$. Similarly, $n(H) \propto \zeta/k_g(H)$, where $k_g(H)$ is the rate coefficient for adsorption of H on to grains. It follows that

$$\frac{n_e}{n(H)} \propto k_g(H) \left(\frac{n_H}{\zeta} \right)^{0.5}$$

and ratios such as $n(C_6H^-)/n(C_6H)$ have the same proportionality. We note that neither k_g nor ζ is well determined in dark clouds, including TMC-1. As water ice forms on grains in regions where the visual extinction, A_v, exceeds a few magnitudes, information on the rate of formation of H_2 derived from observations of diffuse clouds is not applicable. In fact, (H I) observations of the residual atomic hydrogen provide the most direct constraint on k_g in dense clouds.

We neglect reactions with species such as C_2H which can convert C_nH into $C_{n+2}H$ (cf. Millar et al. 2000, 2007). Although these reactions are intrinsically rapid, with rate constants of the order of 10^{-10} cm^3 s^{-1}, they are much slower than electron attachment to C_nH for any reasonable value of the ratio of the abundances of C_2H and e^-. Thus, we believe that we calculate the relative abundances, $n(C_nH^-)/n(C_nH)$, correctly, given the rate coefficients for electron attachment to and detachment from C_nH, but make no such claim for the absolute abundances of these species.

2.2. Grains and PAH

It has been shown that electron attachment to grains and large molecules (which we shall consider to be polycyclic aromatic hydrocarbons, PAH), followed by recombination with positive ions, can have significant effects on the free electron density in molecular clouds (Draine & Sutin 1987; Weingartner & Draine 2001). These processes are particularly important in relation to atomic (as distinct from molecular) ions, whose recombination with electrons in the gas phase is mediated by the emission of a photon and is an intrinsically slow process. In their turn, the abundances of the ions H^+, H_3^+ and HCO^+ affect the ortho:para H_2 ratio, which is crucial in establishing the ortho:para ratios in other species, including the deuterated forms of H_3^+ (Flower et al. 2006a).

Our treatment of the interactions of ions and electrons with grains and PAH follows closely the analysis of Flower & Pineau des Forêts (2003). The existence of PAH in dark molecular clouds is difficult to establish observationally, and their fractional abundance depends on the extent of their accretion on to the grains. There is some indirect evidence (Cardelli et al. 1989) that, in pre-protostellar cores, accretion to and coagulation of grains have occurred prior to the onset of gravitational collapse. In this case, it is likely that PAH will have participated in this process of grain growth. Furthermore, growth occurs differentially, because the rate of accretion is proportional to $n_g(a_g)\pi a_g^2$, where n_g is the grain number density and a_g is the grain radius. An MRN distribution, for example, predicts that $dn_g(a_g)/da_g \propto a_g^{-3.5}$, resulting in faster accretion to smaller grains. We shall suppose that, in the molecular gas from which protostars form, the grains have a mean cross section per hydrogen nucleus $(n_g/n_H)\pi a_g^2 = 1.6 \times 10^{-22}$ cm^2, following accretion and coagulation, and assume that the PAH have been removed, by accretion to the grains, from the gas phase. This reduced value of the grain cross section has been shown to be compatible with the differential freeze-out of carbon- and nitrogen-containing species, and the high levels of deuteration of nitrogen-containing species, which are observed in the early phases of protostellar collapse (Flower et al. 2006b).

In "young" molecular clouds, which may include TMC-1, the process of accretion has had limited time in which to occur. We shall assume that, in such media, the grains follow the MRN distribution, and we shall vary the fractional abundance of PAH between $n_{PAH}/n_H = 10^{-6}$, an upper limit which is consistent with estimates of the fraction of elemental carbon likely to be present in the form of very small gains, and $n_{PAH}/n_H \leq 10^{-8}$, for which the influence of PAH on the fractional ionization of the medium becomes negligible.

3. Results

We have calculated the degree of ionization and the charge distribution, as well as the chemical composition, for conditions which we consider to be typical of the gas from which low-mass stars form. We adopted a density $n_H = 10^4$ cm^{-3} and a kinetic temperature $T = 10$ K. The total rate of ionization and dissociative ionization of H_2 by cosmic rays was taken to be $\zeta = 1 \times 10^{-17}$ s^{-1}, but the effects of adopting a larger value, $\zeta = 5 \times 10^{-17}$ s^{-1}, and a smaller value, $\zeta = 2 \times 10^{-18}$ s^{-1}, were investigated. The chemical network has been discussed by Flower et al. (2006b) and is to be found at `http://massey.dur.ac.uk/drf/protostellar/species_chemistry_06_07`. The results of our calculations of the steady-state abundances are to be found in Tables 1 and 2.

When an MRN distribution is adopted, with grain sizes in the range $0.01 < a_g < 0.3$ μm, a mass density of the grain material $\rho_g = 2$ g cm^{-3}, and a dust:grain mass ratio of 0.0094 (corresponding to our adopted elemental depletions), the mean fractional abundance of the grains is $n_g/n_H = 1.2 \times 10^{-10}$. On the other hand, when it is assumed that the grains have undergone coagulation in the early phases of protostellar collapse and $a_g = 0.5$ μm (Flower et al. 2006b), $n_g/n_H = 2.1 \times 10^{-14}$.

In Table 1, we compare fractional abundances calculated using $\zeta = 1 \times 10^{-17}$ s^{-1} with the values observed towards the nearby prestellar core TMC-1. The observations listed by van Dishoeck et al. (1993) refer to the cyanopolyyne peak, whose density is estimated to be of the order of 10^4 cm^{-3}. TMC-1 is known to be unusually rich in carbon-chain compounds and has often been considered to be considerably younger than other cores in the solar neighbourhood, with an age of the order of 10^5 yr. We give also an estimate of the fractional abundance of atomic hydrogen, based on H I measurements made with the Arecibo radio telescope (Li & Goldsmith 2003; Goldsmith & Li 2005; Goldsmith 2007, personal communication). The spatial resolution of their observations was 0.12 parsec, in regions where the density $n(H_2) \approx 2000$ cm^{-3}. From their observations, we deduce $n(H) \approx 3$ cm^{-3} in TMC-1, and, following the discussion in Sect. 2.1, assume that the density of atomic hydrogen is independent of the total density, n_H.

Table 1. The fractional abundances, $n(\mathrm{X})/n_{\mathrm{H}}$, in steady state at $T = 10$ K, of selected species, X, including large molecules (PAH) and grains. The relative abundances of the carbon-chain molecules, C_4H and C_6H, and their anions, C_4H^- and C_6H^-, are also listed, as are the ortho:para H_2 and H_3^+ ratios. The ratio C_8H^-:C_8H is taken to be the same as C_6H^-:C_6H (see text, Sect. 2.1). In these calculations was adopted a mean grain cross section per hydrogen nucleus, $\langle\sigma\rangle_{\mathrm{g}} \equiv (n_{\mathrm{g}}/n_{\mathrm{H}})\pi a_{\mathrm{g}}^2$, of either $\langle\sigma\rangle_{\mathrm{g}} = 1.6 \times 10^{-22}$ cm^2 or $\langle\sigma\rangle_{\mathrm{g}} = 1.6 \times 10^{-21}$ cm^2; the latter corresponds to an MRN size distribution. The gas density is $n_{\mathrm{H}} = 10^4$ cm^{-3} and the cosmic ray ionization rate is $\zeta = 1 \times 10^{-17}$ s^{-1}. The values observed in TMC-1 are taken from (1) van Dishoeck et al. (1993), (2) Brünken et al. (2007), (3) McCarthy et al. (2006), (4) Li & Goldsmith (2003), Goldsmith & Li (2005). Numbers in parentheses are powers of 10.

Model	1	2	3	4	
	$\langle\sigma\rangle_{\mathrm{g}} = 1.6 \times 10^{-22}$	1.6×10^{-21}	1.6×10^{-21}	1.6×10^{-21} cm^2	TMC-1
$n_{\mathrm{PAH}}/n_{\mathrm{H}} =$	10^{-8}	10^{-8}	10^{-7}	10^{-6}	
C_2H	2.70(−08)	3.94(−08)	5.63(−08)	6.47(−08)	4.0(−08)[1]
C_4H^-:C_4H^0	1.97(−03)	1.15(−02)	6.14(−03)	5.67(−03)	$\lesssim$ 1.4(−04)[2]
C_6H^-:C_6H^0	8.11(−02)	4.65(−01)	1.83(−01)	5.27(−02)	2.5(−02)[3]
C_8H^-:C_8H^0	8.11(−02)	4.65(−01)	1.83(−01)	5.27(−02)	5.0(−02)[2]
PAH^0	6.30(−09)	6.50(−09)	7.88(−08)	9.45(−07)	
PAH^-	3.71(−09)	3.51(−09)	2.12(−08)	5.39(−08)	
g^0	6.38(−15)	7.90(−11)	9.50(−11)	1.10(−10)	
g^-	1.42(−14)	3.81(−11)	2.18(−11)	5.53(−12)	
e^-	3.89(−08)	2.46(−08)	9.35(−09)	2.34(−09)	
H^+	8.29(−09)	5.50(−09)	2.57(−09)	1.09(−09)	
S^+	1.79(−08)	5.40(−09)	1.64(−09)	9.91(−10)	
Fe^+	5.00(−10)	2.30(−10)	7.42(−11)	3.77(−11)	
H_3^+	2.26(−09)	2.33(−09)	2.36(−09)	2.30(−09)	
HCO^+	3.60(−09)	6.08(−09)	1.49(−08)	3.28(−08)	4.0(−09)[1]
DCO^+	3.40(−11)	5.43(−11)	1.46(−10)	5.51(−10)	6.0(−11)[1]
o : p H_2	9.65(−04)	1.22(−03)	1.65(−03)	1.68(−03)	
o : p H_3^+	3.93(−01)	4.53(−01)	5.26(−01)	5.24(−01)	
H^0	2.24(−04)	2.40(−05)	2.37(−05)	2.36(−05)	3.0(−04)[4]

3.1. Charge distribution

The effects of modifying the mean grain cross section per hydrogen nucleus may be assessed by comparing the results for grains which are assumed to have undergone coagulation with those computed assuming an MRN distribution (see Table 1). Because the mean grain cross section is larger when an MRN distribution is adopted, the rates of recombination of atomic ions with negatively charged grains are higher and their fractional abundances are lower. As the fractional abundance of the PAH increases, in the range $10^{-8} \leq n_{\mathrm{PAH}}/n_{\mathrm{H}} \leq 10^{-6}$, the fractional electron density in the gas phase decreases, by about an order of magnitude. When $n_{\mathrm{PAH}}/n_{\mathrm{H}} = 10^{-8}$, the influence of the PAH on the degree of ionization of the gas is small.

The response of the atomic ions H^+ and S^+ may be seen from the corresponding entries in Table 1. Because the ionization potential of H (13.6 eV) is greater than that of S (10.4 eV), H^+ is more readily neutralized in charge transfer reactions with atoms and molecules in the gas phase. The steady-state fractional abundances of the ions H_3^+ and HCO^+ are also listed in this Table. In common with other molecular ions, these species are removed by dissociative recombination with electrons, which is an intrinsically fast process. It follows that the fractional abundances of molecular ions tend to increase with decreasing electron density. However, the proton-transfer reaction of H_3^+ with CO, which is an abundant molecule, i.e.

$$H_3^+ + CO \rightarrow HCO^+ + H_2$$

provides an additional and important channel for the destruction of H_3^+ and the creation of HCO^+, whereas the corresponding proton-transfer reaction of HCO^+ with CO has no chemical effect. Thus, changes in the electron density have a smaller influence on the abundance of H_3^+ than on the abundance of HCO^+.

The variations in the fractional abundances of H^+, H_3^+ and HCO^+ have consequences for the ortho:para (o:p) ratio of H_2, and hence for the o:p ratios of species such as H_3^+. Proton-exchange reactions of the type

$$H^+ + H_2(\mathrm{o}) \rightleftharpoons H^+ + H_2(\mathrm{p})$$

establish the steady-state value of the o:p H_2 ratio. The rate coefficients for the reactions involving H^+ and H_3^+ have similar magnitudes. On the other hand, experimental studies by Huntress (1977) of the reaction $HCO^+(D_2, HD)DCO^+$ suggest that the the corrresponding reaction of HCO^+ with H_2 is insignificant. The tendency for the o:p H_2 ratio to increase with decreasing abundance of H^+ is mitigated by the approximate constancy of the abundance of H_3^+. Consequently, the o:p H_2 ratio increases by less than a factor of 2 between the extreme cases in Table 1. The o:p H_3^+ ratio moves approximately in tandem with that of H_2.

3.2. The diagnostic potential of the ratios $n(C_nH^-)/n(C_nH)$

We mentioned in the Introduction that one of the motivations for the present study was the possibility that the ratios $n(C_nH^-)/n(C_nH)$ might be diagnostics of the degree of ionization of the gas, specifically of the fractional electron abundance. The value of the column density ratio $N(C_6H^-)/N(C_6H)$ observed in TMC-1 is approximately 0.025 (McCarthy et al. 2006) and $N(C_8H^-)/N(C_8H) \approx 0.05$ (Brünken et al. 2007). The latter authors also give an upper limit of 1.4×10^{-4} to the ratio $N(C_4H^-)/N(C_4H)$ in TMC-1.

In their simulation of the conditions in TMC-1, Millar et al. (2007) calculated $n(C_4H^-)/n(C_4H) = 1.94 \times 10^{-3}$, $n(C_6H^-)/n(C_6H) = 8.91 \times 10^{-2}$, and $n(C_8H^-)/n(C_8H) = 5.42 \times 10^{-2}$, in steady state; their computed values are in good agreement with the results reported in the second column of Table 1

(model 1), to which corresponds a low value of the grain cross section per hydrogen nucleus (and hence a low rate of formation of H_2) and a negligible fractional abundance of PAH. The latter condition is compatible with the neglect of PAH in the calculations of Millar et al. (2007). At an "early time" ($t = 3.16 \times 10^5$ yr), when their computed column densities are in much better agreement with observations than at steady state, Millar et al. obtained $n(C_4H^-)/n(C_4H) = 1.23 \times 10^{-3}$, $n(C_6H^-)/n(C_6H) = 5.22 \times 10^{-2}$, and $n(C_8H^-)/n(C_8H) = 4.05 \times 10^{-2}$. The observed values are, respectively, $\lesssim 1.4 \times 10^{-4}$, 2.5×10^{-2} and 5.0×10^{-2}. As noted in Sect. 2.1, the key parameters determining the value of the ratio $n(C_6H^-)/n(C_6H)$ in dark clouds are the electron density and the density of atomic hydrogen. Models with a small mean grain cross section per hydrogen nucleus, $\langle\sigma\rangle_g$, resulting in a low rate of removal of H from the gas phase, yield smaller values of $n(C_6H^-)/n(C_6H)$ for a given fractional abundance of PAH, as may be seen by comparing the results in Cols. 2 and 3 of Table 1. The rate coefficient for removal of H by adsorption to grains is given by

$$k_g(H) = (n_g/n_H)\pi a_g^2 v_{th} s_g(H)$$

where $v_{th} = [8k_BT/(\pi m_H)]^{0.5}$ is the mean thermal speed of the H atoms and $s_g(H)$ is the sticking probability ($s_g = 0.83$ at $T = 10$ K, following Hollenbach & McKee 1979). Adopting an MRN distribution, we obtain $k_g(H) = 5.8 \times 10^{-17}(T/10)^{0.5}$ cm^3 s^{-1}; $k_g(H)$ is 10 times smaller when $a_g = 0.5$ μm is assumed. We note that Goldsmith et al. (2005) adopted $k_g(H) = 1.2 \times 10^{-17}(T/10)^{0.5}$ cm^3 s^{-1} in their analysis of H I observations of molecular clouds, i.e. an approximately 5 times smaller value; we shall return to this point in Sect. 4.

It is instructive to compare the free-fall time, $t_{ff} = 4.3 \times 10^7 n_H^{-0.5}$ yr, where n_H is in units of cm^{-3}, with the H_2 formation time, $t_{form} = [k_g(H)n_H]^{-1}$. In order for molecular hydrogen to be able to form, on grains, in the free-fall time, the density of the gas must satisfy

$$n_H \geq [n_0(t_0k_g)^2]^{-1}$$

where t_0 is the free-fall time corresponding to density n_0. Taking $k_g(H) = 5.8 \times 10^{-17}$ cm^3 s^{-1}, corresponding to an MRN distribution at $T = 10$ K, we obtain $n_H \geq 1.6 \times 10^2$ cm^{-3}. When $a_g = 0.5$ μm, $n_H \geq 1.6 \times 10^4$ cm^{-3}. As a self-gravitating condensation of gas and dust must exist for at least a free-fall time, t_0, these values are not strict lower limits to the density of the gas such that molecular hydrogen has sufficient time to form on the grains.

The timescale for grain coagulation is of the order of 10^5 yr for a gas density $n_H = 10^4$ cm^{-3} (Flower et al. 2005), and so it is possible that limited coagulation has taken place in very young molecular clouds. Accordingly, we have run models in which an MRN grain size distribution was adopted, varying the fractional abundance of PAH in the range $10^{-8} \leq n_{PAH}/nH \leq 10^{-6}$. We consider that the case of a large gas-phase abundance of PAH is the most consistent with the assumption of an MRN size distribution. It may be seen from the results in the final column of Table 1 that the adoption of an MRN distribution, together with a high fractional abundance of PAH, $n_{PAH}/nH = 10^{-6}$, leads to a value of the ratio $n(C_6H^-)/n(C_6H)$ which is within a factor of approximately 2 of that observed by McCarthy et al. (2006). The high PAH abundance results in a low fractional abundance of free electrons and hence smaller fractions of the anions; C_4H^- is less sensitive to the decrease in the free electron fraction than C_6H^- because the rate coefficient for electron attachment to C_4H is lower than for C_6H (see Sect. 2.1), and hence electron transfer from PAH^- is relatively more important for C_4H than C_6H. Thus, whilst a possible explanation of the low value of $n(C_6H^-)/n(C_6H)$ which has been observed in TMC-1 is a low fractional abundance of free electrons (and a high fractional abundance of PAH^-), the computed values of $n(C_4H^-)/n(C_4H)$ for *all* the models in Table 1 remain much larger than the observed upper limit. Furthermore, with a lower fraction of electrons are associated higher fractions of HCO^+ and DCO^+; and, in the limit of $n_{PAH}/nH = 10^{-6}$ (model 4), the fractional abundances of HCO^+ and DCO^+ approach values which are an order of magnitude larger than observed in TMC-1.

An alternative explanation of the observations might be sought in a higher cosmic ray ionization rate. A recent analysis of the formation and destruction of H_3^+ in Galactic molecular clouds (Dalgarno 2006) suggests that the rate of cosmic ray ionization of H_2 could be $\zeta = 5 \times 10^{-17}$ s^{-1}, or even 1×10^{-16} s^{-1}, rather than the canonical value of $\zeta = 1 \times 10^{-17}$ s^{-1}. A larger value of ζ leads to an enhanced fractional abundance of atomic H and hence a higher rate of destruction of C_6H^-. However, in the case of the model in the last column of Table 1, calculations with a five times larger value of $\zeta = 5 \times 10^{-17}$ s^{-1} showed only a 20% reduction in the ratio $n(C_6H^-)/n(C_6H)$: the enhanced rate of destruction of the anion is largely offset by an increase in its rate of formation, owing to a higher abundance of free electrons. In the case of the model in Col. 2 of Table 1, a five-fold increase in the value of ζ results in only a 40% reduction in the ratio $n(C_6H^-)/n(C_6H)$. Furthermore, our calculations, including the energy balance of the medium, have shown that cosmic ray ionization rates $\zeta \gtrsim 5 \times 10^{-17}$ s^{-1} are incompatible with gas kinetic temperatures as low as $T \approx 10$ K, which are believed to prevail in prestellar cores.

In Sect. 2.1, we noted that the ratio $n(C_6H^-)/n(C_6H)$ is given by

$$\frac{n(C_6H^-)}{n(C_6H)} = 4.7 \times 10^2 \frac{n_e}{n(H)}$$

under conditions where electron attachment dominates the formation and electron detachment by H the destruction of the anion. In Fig. 1, we plot the computed relationship, as determined by time-dependent calculations with the initial conditions of the models which evolve to the steady-state compositions in Table 1. It may be seen from Fig. 1 that the theoretical relationship is followed closely, over a full 2 orders of magnitude variation of $n_e/n(H)$. Furthermore, the expression above yields values of $n(C_6H^-)/n(C_6H)$ which are in good agreement with the steady-state results in Table 1.

The corresponding plot of the ratio $n(C_4H^-)/n(C_4H)$ is shown also in Fig. 1. In the case of C_4H, the rate of attachment of free electrons is lower than for C_6H, and consequently the transfer of electrons to C_4H from PAH^- becomes significant in model 4, which has the highest fractional abundance of PAH. The other models conform to the relationship

$$\frac{n(C_4H^-)}{n(C_4H)} = 11.2 \frac{n_e}{n(H)},$$

expected in the limit in which the attachment of free electrons dominates the formation, and reactions with H the destruction, of C_4H^-. Applying this and the corresponding formula for $n(C_6H^-)/n(C_6H)$, and using the observed value of C_6H^-:C_6H, we would expect a ratio C_4H^-:C_4H in TMC-1 of 6×10^{-4}. Adopting the observed value of C_4H:H_2 from van Dishoeck et al. (1993), the predicted abundance of C_4H^-, relative to H_2, is $n(C_4H^-)/n(H_2) = 1.2 \times 10^{-11}$.

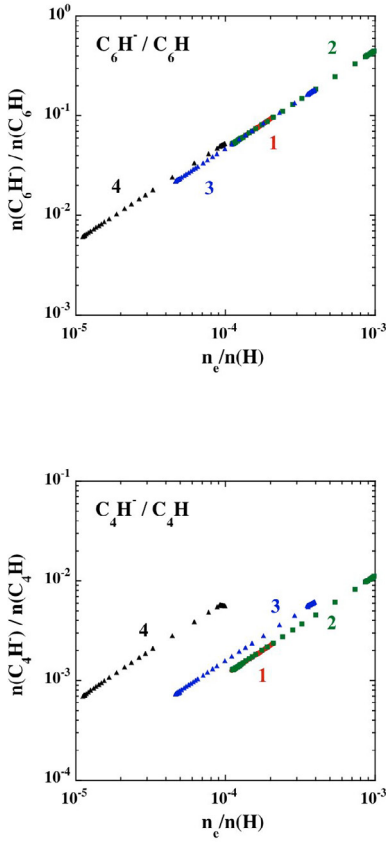

Fig. 1. The ratios $n(C_6H^-)/n(C_6H)$ and $n(C_4H^-)/n(C_4H)$ as functions of n_e/n_H, derived from time-dependent calculations, starting from the initial conditions of the models in Table 1 (which are denoted "1" to "4", from left to right in the table).

Given the proportionality between $n(C_6H^-)/n(C_6H)$ and $n_e/n(H)$ and that

$$\frac{n_e}{n(H)} \propto k_g(H)\left(\frac{n_H}{\zeta}\right)^{0.5}$$

(see Sect. 2.1), a more empirical approach to establishing the fractional electron density suggests itself. As already mentioned, the rate of cosmic ray ionization of H_2, ζ, and of adsorption of H on to grains, $k_g(H)$, in TMC-1 are uncertain. A simultaneous reduction in the values of both these parameters, to $k_g(H) = 1.2\times10^{-18}$ cm^3 s^{-1} (other parameters being the same as in model 1 of Table 1) and $\zeta = 2\times10^{-18}$ s^{-1}, yields the results given in Table 2. Although these parameters might be considered extreme, they produce the best overall agreement with the observations of TMC-1. The fractional abundance of atomic H remains close to the observed value, whilst the electron density is reduced relative to model 1 of Table 1, hence reducing also the calculated value of the ratio C_6H^-:C_6H to a value more consistent with observation. Both the cosmic ray ionization rate and the H_2 formation rate are much lower than assumed in 'standard' models of interstellar chemistry. However, we note that it is quite possible that both parameters vary with position in dense clouds [see, for example, the discussion in Padoan and Scalo (2005) of the cosmic ray flux]. One consequence of such low values of ζ and $k_g(H)$ is that the timescale for reaching chemical equilibrium increases, making it more probable that, in sources like TMC-1, deviations from steady state occur; but this should not change greatly the estimate of the electron density, $n_e/n_H = 1\times10^{-8}$, from Table 2, as the timescale for the fractional ionization (and also the ratios C_nH^-:C_nH) to approach steady state (10^4 yr) remains shorter than the timescale to reach chemical equilibrium; it is also much smaller than the free-fall and grain-coagulation timescales, which are of the order of 10^5 yr in gas of density $n_H = 10^4$ cm^{-3}, as was mentioned earlier in this sub-Section, and the "early time" ($t = 3.16\times10^5$ yr) of Millar et al. (2007).

Table 2. The fractional abundances, $n(X)/n_H$, in steady state at T = 10 K, of selected species, X, including large molecules (PAH) and grains. The relative abundances of the carbon-chain molecules, C_4H and C_6H, and their anions, C_4H^- and C_6H^-, are also listed, as are the ortho:para H_2 and H_3^+ ratios. The ratio C_8H^-:C_8H is taken to be the same as C_6H^-:C_6H (see text, Sect. 2.1). In these calculations, we adopted $k_g(H) = 1.2\times10^{-18}$ cm^3 s^{-1} and $\zeta = 2\times10^{-18}$ s^{-1}. The gas density is $n_H = 10^4$ cm^{-3} and the fractional abundance of PAH is $n_{PAH}/n_H = 10^{-8}$. The values observed in TMC-1 are taken from (1) van Dishoeck et al. (1993), (2) Brünken et al. (2007), (3) McCarthy et al. (2006), (4) Li & Goldsmith (2003), Goldsmith & Li (2005). Numbers in parentheses are powers of 10.

	Calculated	Observed in TMC-1
C_2H	2.55(−08)	4.0(−08)[1]
C_4H^-:C_4H^0	5.69(−04)	$\lesssim$1.4(−04)[2]
C_6H^-:C_6H^0	2.25(−02)	2.5(−02)[3]
C_8H^-:C_8H^0	2.25(−02)	5.0(−02)[2]
PAH^0	6.29(−09)	
PAH^-	3.72(−09)	
g^0	5.31(−15)	
g^-	1.50(−14)	
e^-	1.05(−08)	
H^+	1.85(−09)	
S^+	5.97(−09)	
Fe^+	1.74(−10)	
H_3^+	4.83(−10)	
HCO^+	2.91(−09)	4.0(−09)[1]
DCO^+	2.94(−11)	6.0(−11)[1]
o : p H_2	8.31(−04)	
o : p H_3^+	3.74(−01)	
H^0	2.20(−04)	3.0(−04)[4]

4. Concluding remarks

An important conclusion of our study is that the measurement of abundance ratios such as C_6H^-:C_6H should enable improved estimates to be made of the electron density in molecular clouds, such as TMC-1. There are implications for the rate of cosmic ray ionization of H_2 and the rate of adsorption of atomic H on to grains, although we cannot claim to have established the values of these parameters unambiguously. Previous methods of determining the fractional ionization, which relied on measuring and summing the abundances of positive ions, suffer from the lack of observational information on atomic ions, such as S^+, whose abundance may represent a significant fraction of the total. The ratio $n(C_6H^-)/n(C_6H)$, on the other hand, is directly proportional to $n_e/n(H)$.

When determining electron density and cosmic ray ionization rate, as discussed above, we predict simultaneously several relevant fractional abundances, or abundance ratios, which can be verified observationally: the abundances of HCO^+, DCO^+, and atomic hydrogen, as well as the ratios C_6H^-:C_6H and C_4H^-:C_4H. Our approach requires that these species should coexist; in the case of TMC-1, this assumption is validated by the observational studies of Pratap et al. (1997) and Fossé et al. (2001). Our most successful model is that in Table 2, which has

low values of both the cosmic ray ionization rate and the H_2 formation rate. Unfortunately, the rarity of molecular clouds such as TMC-1, in which carbon-chain molecules like C_6H have an appreciable abundance, will limit the applicability of our method; TMC-1 may be atypically young, as suggested by pseudo-time-dependent chemical models, which yield better agreement with its observed composition at "early times" than in the limit of a steady state (cf. Millar et al. 2000). Furthermore, knowledge of the atomic H abundance is required in order to deduce the electron density.

It has been known since the discovery of 21 cm H I "self-absorption" (Knapp 1974) that the residual atomic hydrogen in molecular clouds is detectable; more recent studies by Li & Goldsmith (2003) and Goldsmith & Li (2005) have confirmed that this is the case. Their observations were made with 3 arcmin resolution (0.12 parsec at the distance of Taurus molecular cloud) and refer to clumps of gas with densities of a few thousand cm^{-3} and typically 5 mag of visual extinction. From measurements of the "H I narrow self-absorption", Goldsmith et al. (2007) have deduced clump ages of the order of 10 Myr, which must be a lower limit to age of the associated molecular cloud. Their study is relevant to the controversy concerning the ages of molecular clouds (see, for example, Ballesteros-Paredes & Hartmann 2007; Tassis & Mouschovias 2004; Hartmann 2003; Palla & Stahler 2002), for which estimates vary in the range $1 \lesssim t \lesssim 30$ Myr.

The analysis of H I line profiles by Goldsmith et al. (2007), which suggests that the higher age estimates are correct, depends on the values which they assumed for the rate of cosmic-ray destruction of H_2, ζ_{CR}[2], and its rate of formation on grains, $n_H k_g(H)$. As noted in Sect. 3.2, the value of $k_g(H)$ which they adopted is approximately 5 times smaller than predicted by an MRN size distribution. The timescale, $[n_H k_g(H)]^{-1}$, implied by the rate coefficient for H_2 formation used in the model of Table 2 is 7 Myr for $n_H \approx 4000$ cm^{-3} inferred for the region in which self-absorbed H I is observed; this is of the same order as the estimations of cloud ages mentioned above. In order to observe directly the pre-protostellar cores in the cloud, an angular resolution of 1 arcmin (0.04 parsec at the distance of Taurus) or less is required; this may be achievable with future instruments, such as the square kilometer array.

Appendix A: "Secondary" photoprocesses

The significance of the ultraviolet radiation field, produced as a consequence of cosmic ray ionization of hydrogen and secondary electron emission, was demonstrated first by Prasad & Tarafdar (1983). Subsequently, detailed calculations of photoionization and photodissociation rates were performed by Gredel et al. (1987, 1989). These authors expressed the rate, per unit volume of gas, of ionization or dissociation of the species X by the "secondary" radiation field in the form

$$R_X = \zeta n(X) \int \frac{\sigma_X(\nu) P(\nu)}{\sigma_{tot}(\nu)} d\nu \qquad (A.1)$$

where $n(X)$ is the number density of the species X, $\sigma_X(\nu)$ is the photoionization or photodissociation cross section at frequency ν, $P(\nu)d\nu$ is the probability that an ultraviolet photon is emitted at this frequency, and

$$\sigma_{tot}(\nu) = \frac{n_g}{n_H}\sigma_g(1-\omega) + \sum_X \frac{n(X)}{n_H}\sigma_X(\nu) \qquad (A.2)$$

is the total cross section for absorption of ultraviolet photons by the grains and by the atoms and molecules in the gas; ω is the grain albedo.

In Eq. (A.1), ζ is the "total" cosmic ray ionization rate, expressed in s^{-1}. Equation (A.1) may be rewritten in the form

$$R_X = \zeta n(H_2) \frac{n_H}{n(H_2)} \frac{n(X)}{n_H} p_X \qquad (A.3)$$

where p_X is the integral in Eq. (A.1). Thus, if ζ is the sum of the rates of ionization and dissociative ionization of H_2 (the reactions displayed in Sect. 1), $\zeta n(H_2)$ is the rate of production, per unit volume of gas, of the secondary electrons which give rise to the ultraviolet radiation field. Referring to Eqs. (A.1) and (A.2), it will be seen that

$$\begin{aligned} \frac{n(X)}{n_H} p_X &= \frac{n(X)}{n_H} \int \frac{\sigma_X(\nu) P(\nu)}{\sigma_{tot}(\nu)} d\nu \\ &= \int \frac{n(X)\sigma_X(\nu)}{n_g\sigma_g(1-\omega) + \sum_X n(X)\sigma_X(\nu)} P(\nu) d\nu \end{aligned} \qquad (A.4)$$

is the efficiency with which a photon will dissociate or ionize species X. It follows that, in order to be consistent with our definition of $\zeta n(H_2)$, as the rate of production, per unit volume of gas, of the secondary electrons, we must define

$$\begin{aligned} r_X &= \zeta n(H_2) \frac{n(X)}{n_H} p_X \\ &= R_X \frac{n(H_2)}{n_H} \end{aligned} \qquad (A.5)$$

as the rate, per unit volume, of dissociation or ionization of the species X by the secondary radiation field; in molecular clouds, $n(H_2)/n_H \approx 1/2$.

When an MRN size distribution is adopted, the main contributions to σ_{tot} (Eq. (A.2)) arise from the grains and, depending on its fractional abundance, from CO. Gredel et al. (1987) computed the photodissociation efficiency of CO, p_{CO}, as a function of the grain albedo, ω, the kinetic temperature of the gas, T, and the fractional abundance of CO, $n(CO)/n_H = 7.5 \times 10^{-5}$, 7.5×10^{-6}, 7.5×10^{-7}. For $T = 10$ K and $\omega = 0.5$, which are the values of these parameters adopted in the calculations below, the corresponding photodissociation probabilities are $p_{CO} = 7$, 12, 14. These results are consistent with the contributions of CO and the dust to σ_{tot} being approximately equal when $n(CO)/n_H = 7.5 \times 10^{-5}$, and the contribution of CO being negligible (of the order of 1%) when $n(CO)/n_H = 7.5 \times 10^{-7}$. We recall that, in the calculations of Gredel et al. (1987), the contribution of the dust to σ_{tot} was 1×10^{-21} cm^2 for an albedo $\omega = 0.5$. On the other hand, when $(n_g/n_H)\pi a_g^2 = 1.6 \times 10^{-22}$ cm^2, the contribution of the dust to σ_{tot} is only 0.8×10^{-22} cm^2 for the same value of ω. Under these latter conditions, absorption by CO exceeds absorption by the dust by about an order of magnitude when $n(CO)/n_H = 7.5 \times 10^{-5}$.

In Table A.1, we summarize our findings regarding the CO photodissociation efficiency, p_{CO}. In our calculations, $n(CO)/n_H = 8.0 \times 10^{-5}$, and the results in Table A.1 indicate that the CO photodissociation efficiency increases by a factor of 13/7 when $(n_g/n_H)\sigma_g = 2 \times 10^{-21}$ cm^2 (Gredel et al. 1987)

[2] Goldsmith et al. (2007) define ζ_{CR} as the rate of destruction of H_2 by cosmic rays; it is equivalent to 2.5ζ, where ζ is the rate of cosmic ray ionization of H_2, as defined in Appendix A. Their expression for k'_{H_2}, the rate coefficient for formation of H_2 on grains, is equivalent to $k_g(H)$ above.

Table A.1. Values of the CO photodissociation efficiency, $p_{\rm CO}$, as calculated by Gredel et al. (1987) for the case of a mean grain cross section per hydrogen nucleus $\langle\sigma\rangle_{\rm g} \equiv (n_{\rm g}/n_{\rm H})\sigma_{\rm g} = 2 \times 10^{-21}$ cm^2, and as deduced from their results for the case of $\langle\sigma\rangle_{\rm g} = 1.6 \times 10^{-22}$ cm^2. A dust albedo $\omega = 0.5$ and a gas temperature $T = 10$ K have been adopted.

$n({\rm CO})/n_{\rm H}$	$\langle\sigma\rangle_{\rm g} = 2 \times 10^{-21}$	1.6×10^{-22} cm^2
7.5×10^{-5}	7	13
7.5×10^{-6}	12	76
7.5×10^{-7}	14	150

is replaced by $(n_{\rm g}/n_{\rm H})\sigma_{\rm g} = 1.6 \times 10^{-22}$ cm^2, corresponding to grains which have already undergone coagulation. If CO is the main contributor to the sum over species, X, appearing in the expression (Eq. (A.2)) for $\sigma_{\rm tot}(\nu)$, the photodissociation and photoionization probabilities of the other species also increase by this same factor of approximately 2.

In the models presented above, we investigate the influence of PAH on the distribution of charge in the medium. Following Verstraete & Léger (1992, Fig. 4), we take a mean absorption cross section $\sigma_{\rm PAH} \approx 5 \times 10^{-18} N_{\rm C}$ cm^2, where $N_{\rm C}$ is the number of carbon atoms in the PAH, for the range of wavelengths $\lambda \gtrsim 100$ nm over which the secondary photons are emitted. Then, the contribution of the PAH to $\sigma_{\rm tot}$ is $2.7 \times 10^{-16} n_{\rm PAH}/n_{\rm H}$ cm^2 for our representative PAH, $C_{54}H_{18}$ ($N_{\rm C} = 54$). The fractional abundance of the PAH is limited by the availability of carbon, and $n_{\rm PAH}/n_{\rm H} \leq 10^{-6}$ is a reasonable upper limit, which corresponds to 15% of the elemental carbon being in the form of PAH. In this case, the contribution of the PAH to $\sigma_{\rm tot}$ is approximately 13% for an MRN distribution, $\omega = 0.5$, $T = 10$ K, and $n({\rm CO})/n_{\rm H} = 7.5 \times 10^{-5}$. If the grains have undergone coagulation, it seems probable that the PAH will have been depleted from the gas phase, and $n_{\rm PAH}/n_{\rm H} \ll 10^{-6}$; in this case, their contribution to $\sigma_{\rm tot}$ is negligible.

Acknowledgements. This work has been been partially supported by the EC Marie-Curie Research Training Network "The Molecular Universe". We are grateful to Eric Herbst for information relating to the probabilities of electron attachment to carbon-chain molecules and to Paul Goldsmith for information relating to his H I observations. We thank Paola Caselli for perceptive comments on an earlier version of this paper.

References

Ballesteros-Paredes, J., & Hartmann, L. 2007 Rev. Mex. Astron. Astrofis., 43, 123
Barckholtz, C., Snow, T. P., & Bierbaum, V. M. 2001, ApJ, 547, L171
Brünken, S., Gupta, H., Gottlieb, C. A., McCarthy, M. C., & Thaddeus, P. 2007, ApJ, 664, L43
Cardelli, J. A., Clayton, G. C., & Mathis, J. S. 1989, ApJ, 345, 245
Caselli, P., Walmsley, C. M., Terzieva, R., & Herbst, E. 1998, ApJ, 499, 234
Cernicharo, J., Guélin, M., Agúndez, M., et al. 2007, A&A, 467, L37
Cravens, T. E., & Dalgarno, A. 1978, ApJ, 219, 750
Dalgarno, A. 2006, Proc. Nat. Acad. Sci., 103, 12269
Draine, B. T., & Sutin, B. 1987, ApJ, 320, 803
Flower, D. R., & Pineau des Forêts, G. 2003, MNRAS, 343, 390
Flower, D. R., Pineau des Forêts, G., & Walmsley, C. M. 2005, A&A, 436, 933
Flower, D. R., Pineau des Forêts, G., & Walmsley, C. M. 2006a, A&A, 449, 621
Flower, D. R., Pineau des Forêts, G., & Walmsley, C. M. 2006b, A&A, 456, 215
Fossé, D., Cernicharo, J., Gerin, M., & Cox, P. 2001, ApJ, 552, 168
Goldsmith, P. F., & Li, D. 2005, ApJ, 622, 938
Goldsmith, P. F., Li, D., & Krco, M. 2007, ApJ, 654, 273
Gredel, R., Lepp, S., & Dalgarno, A. 1987, ApJ, 323, L137
Gredel, R., Lepp, S., Dalgarno, A., & Herbst, E. 1989, ApJ, 347, 289
Hartmann, L. 2003, ApJ, 585, 398
Hollenbach, D. J., & McKee, C. F. 1979, ApJS, 41, 555
Huntress, W. T. 1977, ApJS, 33, 495
Knapp, G. R. 1974, AJ, 79, 527
Li, D., & Goldsmith, P. F. 2003, ApJ, 585, 823
Mathis, J. S., Rumpl, W., & Nordsieck, K. H. 1977, ApJ, 217, 425
McCarthy, M. C., Gottlieb, C. A., Gupta, H., & Thaddeus, P. 2006, ApJ, 652, L141
Millar, T. J., Herbst, E., & Bettens, R. P. A. 2000, MNRAS, 316, 195
Millar, T. J., Walsh, C., Cordiner, M. A., Ní Chuimín, R., & Herbst, E. 2007, ApJ, 662, L87
Modelli, A., & Mussoni, L. 2007, Chem. Phys., 332, 367
Morris, M., Turner, B. E., Palmer, P., & Zuckerman, B. 1976, ApJ, 205, 82
Ossenkopf, V. 1993, A&A, 280, 617
Ossenkopf, V., & Henning, Th. 1994, A&A, 291, 943
Padoan, P., & Scalo, J. 2005, ApJ, 624, L97
Palla, F., & Stahler, S. W. 2002, ApJ, 581, 1194
Prasad, S. S., & Tarafdar, S. P. 1983, ApJ, 267, 603
Pratap, P., Dickens, J. E., & Snell, R. L., et al. 1997, ApJ, 486, 862
Remijan, A. J., Hollis, J. M., & Lovas, F. J., et al. 2007, ApJ, 664, L47
Suttner, G., & Yorke, H. W. 2001, ApJ, 551, 461
Tassis, K., & Mouschovias, T. Ch. 2004, ApJ, 616, 283
Taylor, T. R., Xu, C., & Neumark, D. M. 1998, J. Chem. Phys., 108, 10018
Terzieva, R., & Herbst, E. 2000, Int. J. Mass Spectrom., 201, 135
van Dishoeck, E. F., Blake, G. A., Draine, B. T., & Lunine, J. I. 1993, in Protostars and Planets III, eds. E. H. Levy & J. I. Lunine (University of Arizona Press), 163
Verstraete, L., & Léger, A. 1992, A&A, 266, 513
Weingartner, J. C., & Draine, B. T. 2001, ApJ, 548, 296